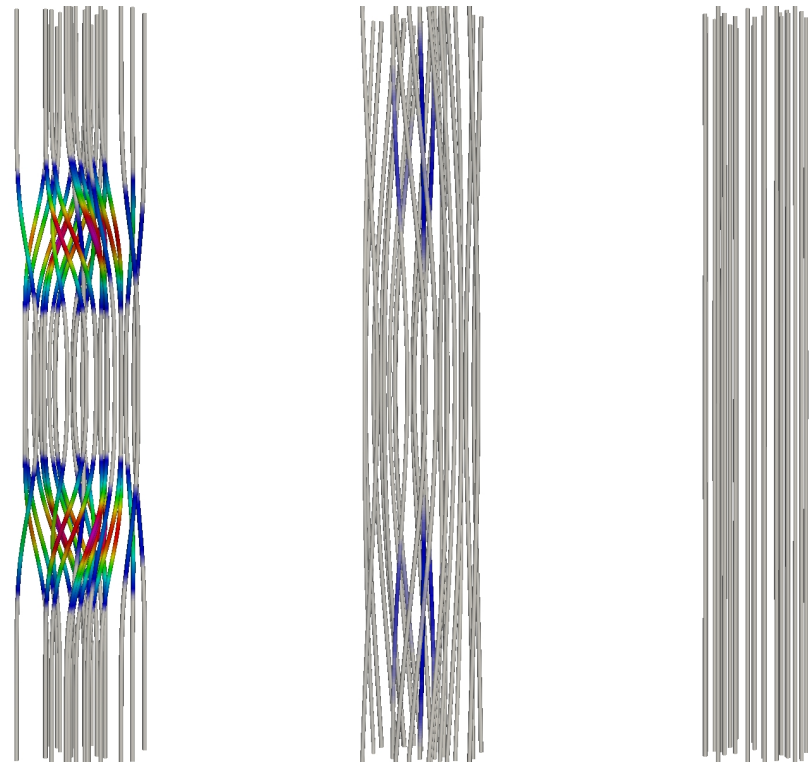


# Ideal magnetic field relaxation and mimetic numerical operators

Simon Candelaresi



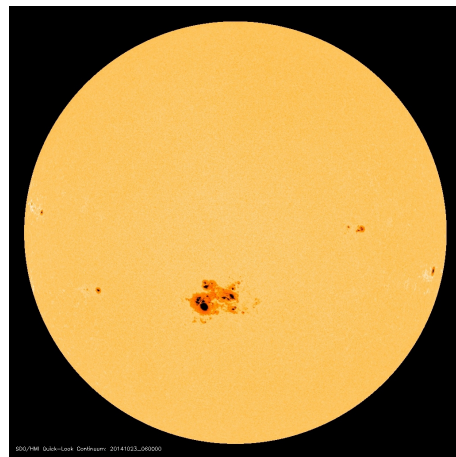
[simon.candelaresi@gmail.com](mailto:simon.candelaresi@gmail.com)

# Overview

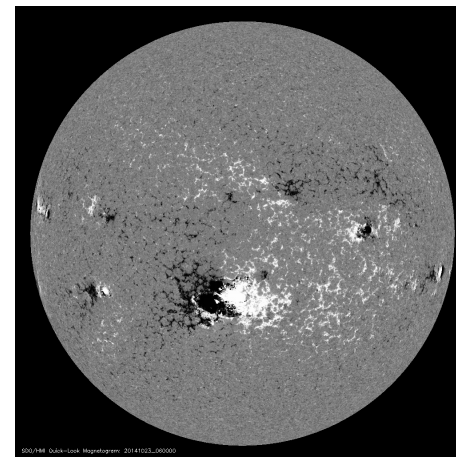
1. Physical Motivation
2. Magnetic Field Topology and Evolution
3. Force-Free Relaxation
4. Mimetic Methods
5. Latest Developments on Field Relaxation

# Magnetic Fields in the Universe

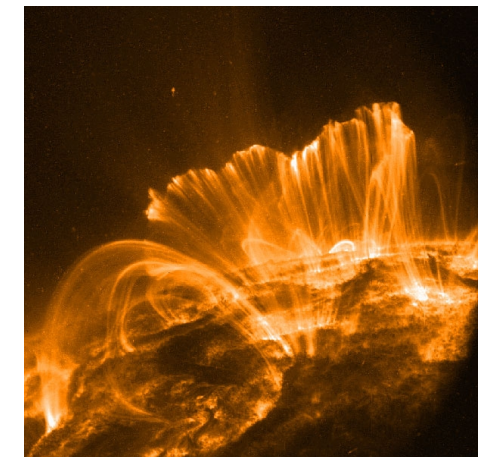
Sun:  
2-2,000G



Continuum  
2014-10-23 (NASA)

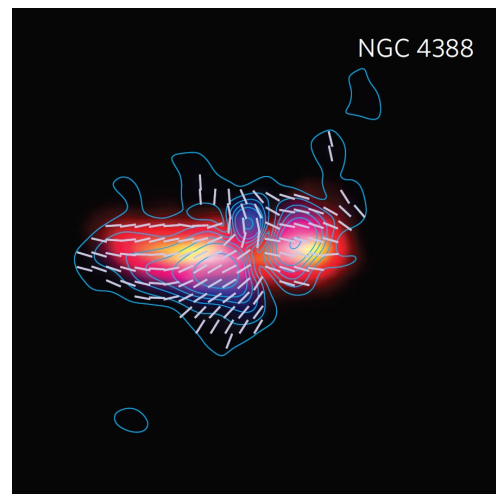


HMI (magnetic field)  
2014-10-23 (NASA)



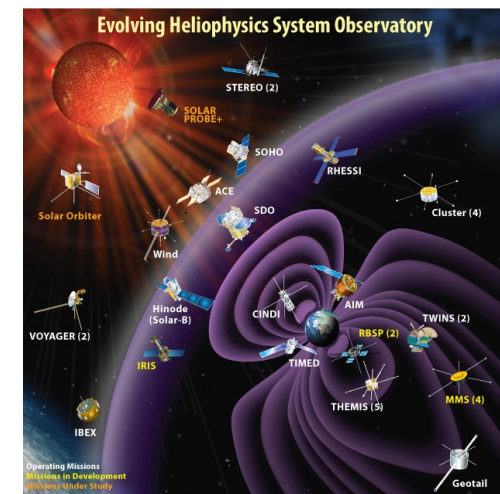
Coronal Loops (NASA)

Galaxies:  
 $10e-6$  G



Pfrommer (2010)  
DOI: 10.1038/NPHYS1657

Earth:  
0.1-1G



NASA

# Field's Environment

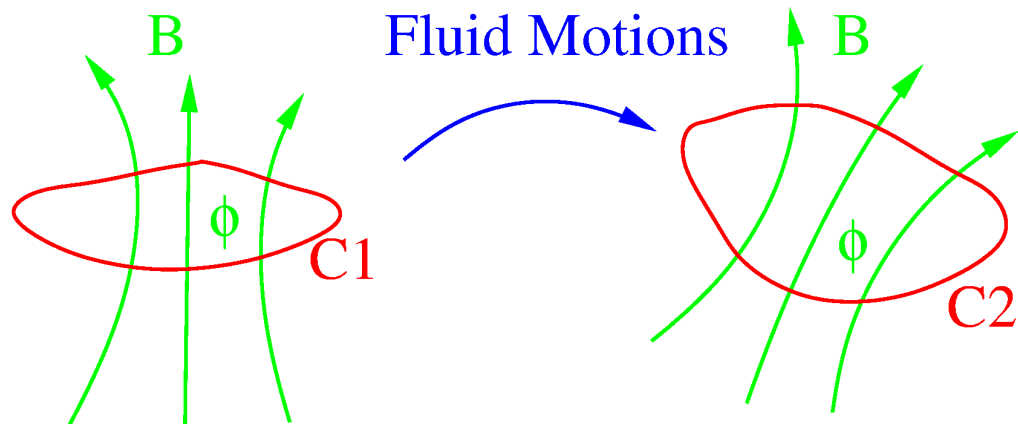
Magnetically dominated:  
magnetic pressure  $\gg$  thermal pressure

$$B^2/(2\mu_0) \gg nk_B T$$

$$\beta = 2\mu_0 \frac{nk_B T}{B^2} \ll 1 \quad \text{Solar corona: } \beta \approx 0.01$$

Frozen-in magnetic flux:  
magnetic resistivity small:  $t_{\text{dissipation}} \gg t_{\text{dynamical}}$

→ Magnetic field is *frozen-in* to the fluid.



Batchelor (1950)  
DOI: 10.1098/rspa.1950.0069

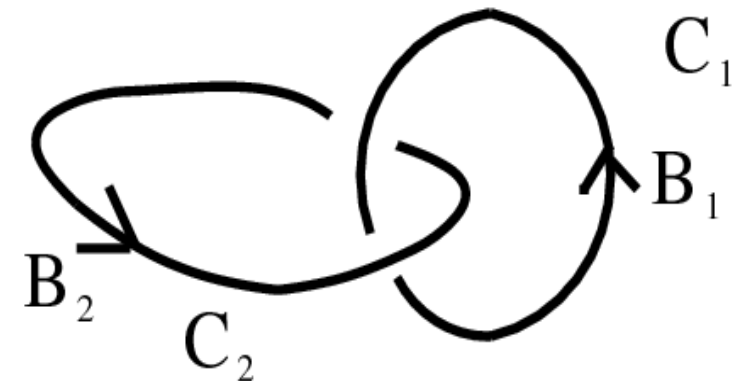
# Magnetic Field Topology

Measure for the topology:

$$H_M = \int_V \mathbf{A} \cdot \mathbf{B} \, dV = 2n\phi_1\phi_2$$

$$\nabla \times \mathbf{A} = \mathbf{B} \quad \phi_i = \int_{S_i} \mathbf{B} \cdot d\mathbf{S}$$

$n$  = number of mutual linking



*Moffatt (1969)*  
DOI: 10.1017/S0022112069000991

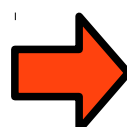
Conservation of magnetic helicity:

$$\lim_{\eta \rightarrow 0} \frac{\partial}{\partial t} \langle \mathbf{A} \cdot \mathbf{B} \rangle = 0 \quad \eta = \text{magnetic resistivity}$$

Realizability condition:

$$E_m(k) \geq k|H(k)|/2\mu_0$$

*Arnold (1974)*



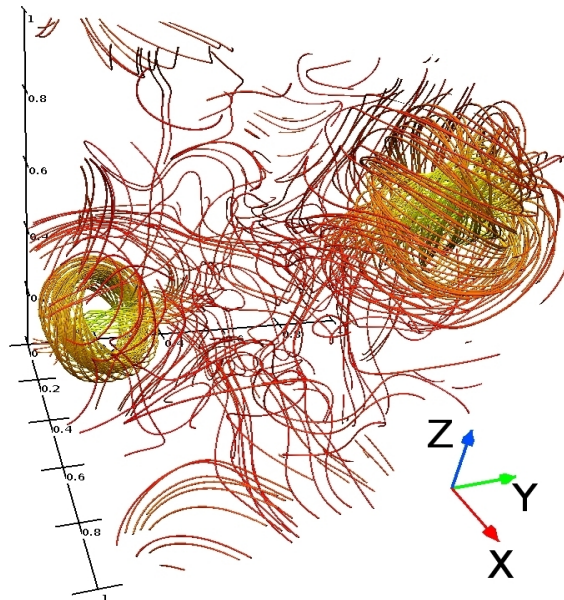
Magnetic energy is bound from below by magnetic helicity.

# Relaxation of Magnetic Fields

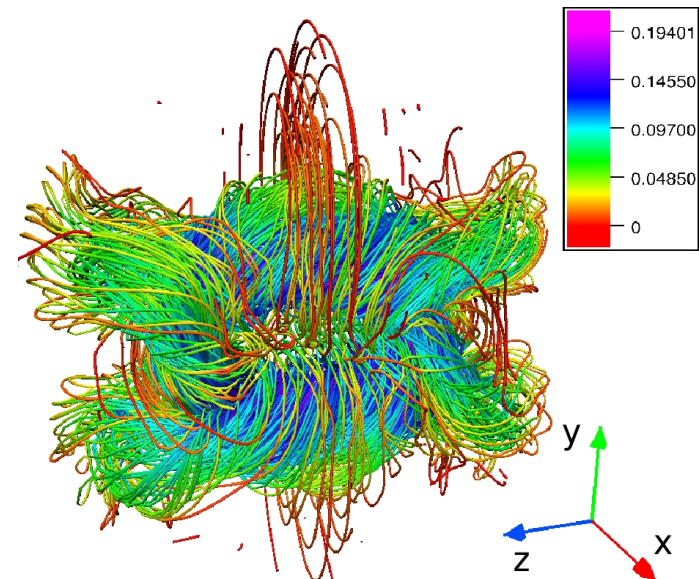
Global magnetic helicity conservation

→ final state is linearly force-free:  $\nabla \times \mathbf{B} = \alpha \mathbf{B}$

*Woltjer (1958)*  
DOI: [10.1073/pnas.44.9.833](https://doi.org/10.1073/pnas.44.9.833)



*Candelaresi (2011)*  
DOI: [10.1103/PhysRevE.84.016406](https://doi.org/10.1103/PhysRevE.84.016406)



*Del Sordo (2010)*  
DOI: [10.1103/PhysRevE.81.036401](https://doi.org/10.1103/PhysRevE.81.036401)

# Taylor Relaxation

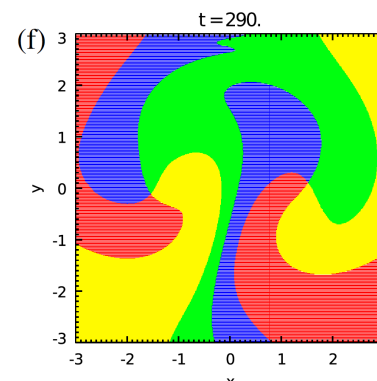
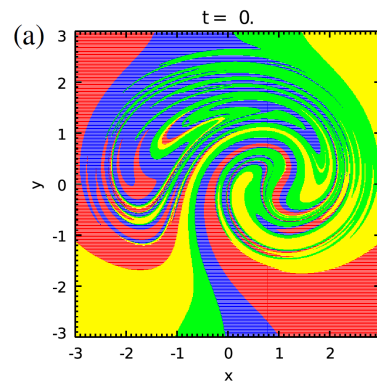
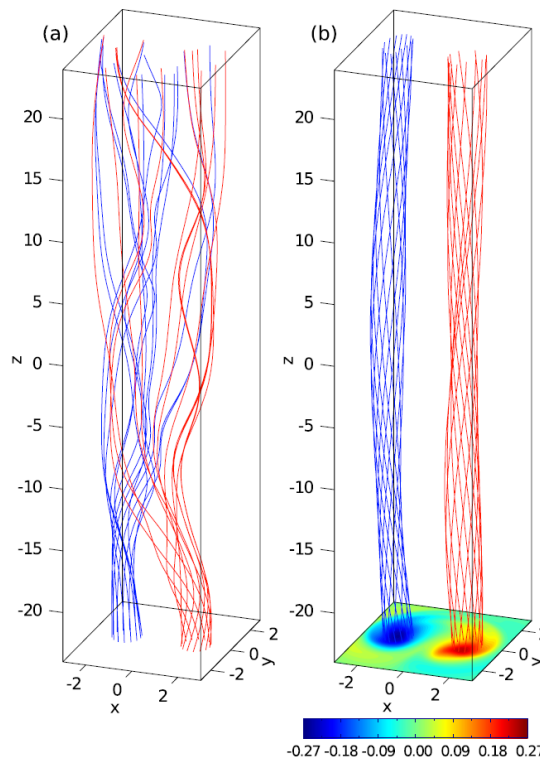
Field line magnetic helicity conservation

→ final state is non-linear force-free:  $\nabla \times \mathbf{B} = \lambda(a, b)\mathbf{B}$

*Taylor (1974)*

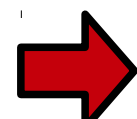
*DOI: 10.1103/PhysRevLett.33.1139*

Does the system always reach this state?



*Yeates (2010)*

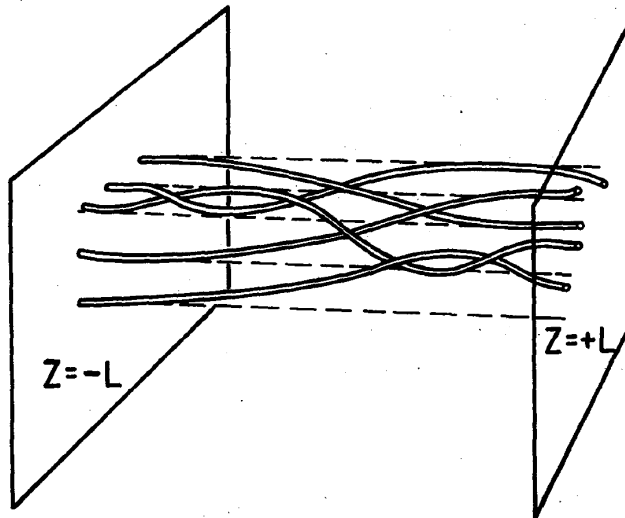
*DOI: 10.1103/PhysRevLett.105.085002*



Not necessarily. Additional topological degree must be conserved.

# Parker Conjecture

Line-tied magnetic field bound within two plates.



*Parker (1972)*  
*DOI: 10.1086/151512*

- Hydrostatic equilibrium only if field variation is uniform along the field.
- If equilibrium is not reached field lines merge and magnetic energy is dissipated (topological dissipation).
- For complex topologies formation of singular current sheets.

# Force-Free Magnetic Fields

Solar corona: low plasma beta and magnetic resistivity

→ Force-free magnetic fields

→ Minimum energy state

$$(\nabla \times \mathbf{B}) \times \mathbf{B} = 0 \Leftrightarrow \nabla \times \mathbf{B} = \alpha \mathbf{B}$$

$$\mathbf{B} \cdot \nabla \alpha = 0 \quad \text{Beltrami field}$$

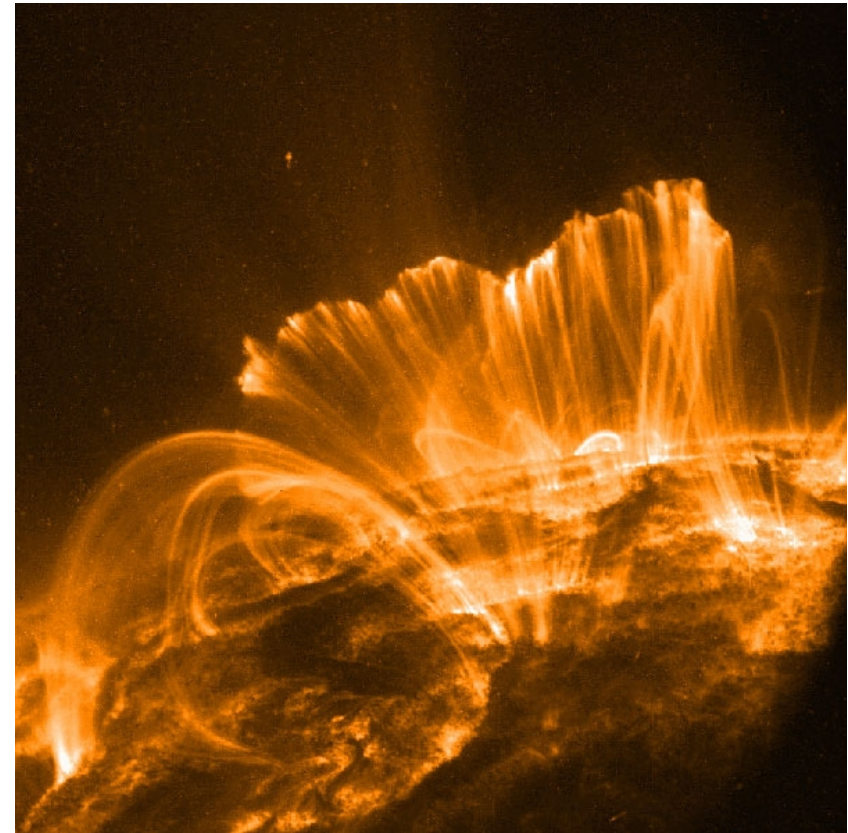
Problem:

Find a force-free state for a magnetic field with given topology.

Current sheets?

Here:

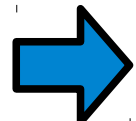
Numerical method for finding such states.



NASA

# Ideal Field Relaxation

Ideal induction eq.:  $\frac{\partial \mathbf{B}}{\partial t} - \nabla \times (\mathbf{u} \times \mathbf{B}) = 0$



Frozen in magnetic field.

(Batchelor, 1950)



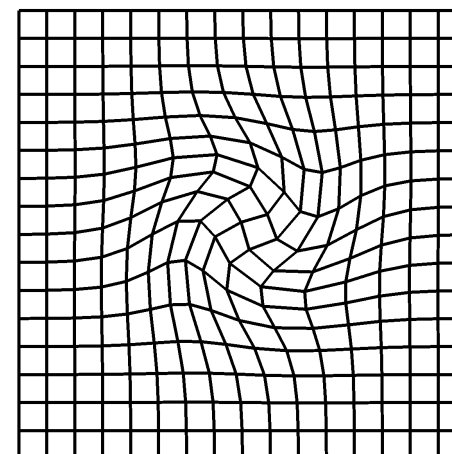
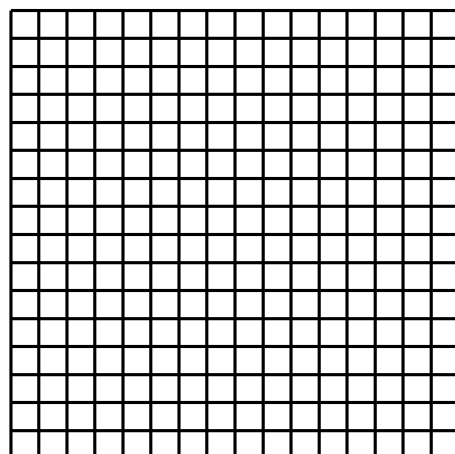
**But:** Numerical diffusion in finite difference Eulerian codes.



**Solution:** Lagrangian description of moving fluid particles:

$$\mathbf{x}(\mathbf{X}, 0) = \mathbf{X}$$

$$\mathbf{x}(\mathbf{X}, t)$$



# Ideal Field Relaxation

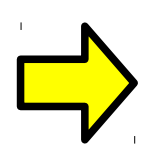
Field evolution:  $B_i(\mathbf{X}, t) = \frac{1}{\Delta} \sum_{j=1}^3 \frac{\partial x_i}{\partial X_j} B_j(\mathbf{X}, 0)$

$$\Delta = \det \left( \frac{\partial x_i}{\partial X_j} \right)$$

Preserves topology and divergence-freeness.

Grid evolution:  $\frac{\partial \mathbf{x}(\mathbf{X}, t)}{\partial t} = \mathbf{u}(\mathbf{x}(\mathbf{X}, t), t)$

Magneto-frictional term:  $\mathbf{u} = \gamma \mathbf{J} \times \mathbf{B}$        $\mathbf{J} = \nabla \times \mathbf{B}$


$$\frac{dE_M}{dt} < 0$$

(Craig and Sneyd 1986)

# Numerical Curl Operator

Compute  $\mathbf{J} = \nabla \times \mathbf{B}$  on a distorted grid:

$$\frac{\partial B_i}{\partial x_j} = X_{\alpha,j} (x_{i,\alpha\beta} B_\beta^0 \Delta^{-1} + x_{i,\beta} B_{\beta,\alpha}^0 \Delta^{-1} - x_{i,\beta} B_\beta^0 \Delta^{-2} \Delta_{,\alpha})$$

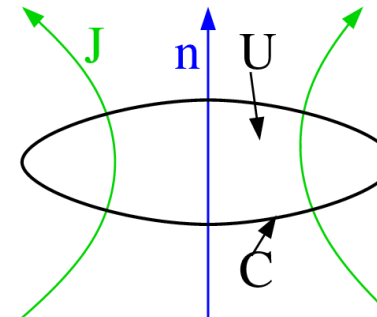
$$B_i^0 = B_i(0)$$

(*Craig and Sneyd 1986*)

-  Multiplication of several terms leads to high numerical errors.
-  Current not divergence free:  $\nabla \cdot \mathbf{J} \neq 0$
-  Only reaching a certain force-freeness. (*Pontin et al. 2009*)

# Mimetic Numerical Operators

$$I = \int_U \mathbf{J} \cdot \mathbf{n} \, dS = \oint_C \mathbf{B} \cdot d\mathbf{r}$$



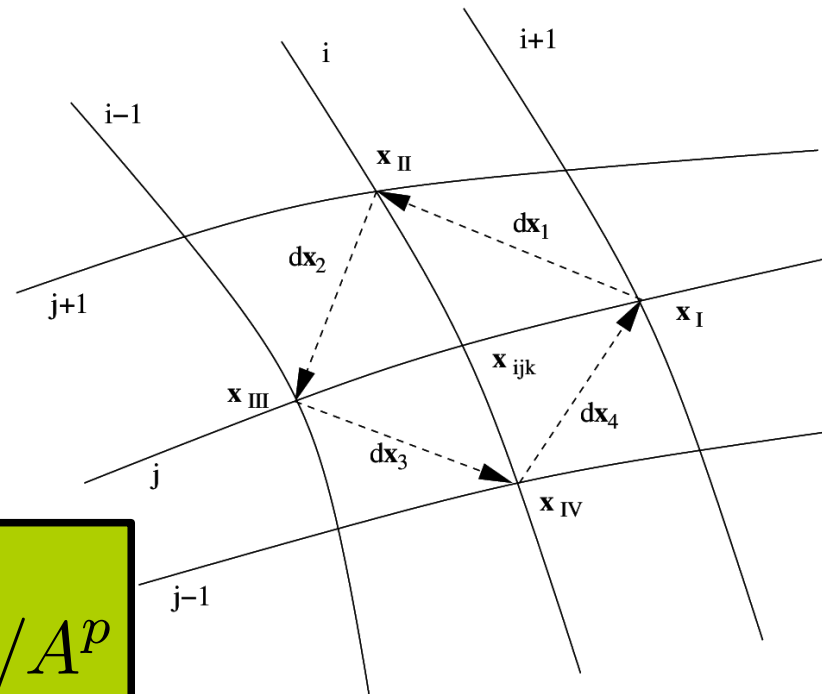
Discretized:

$$I \approx \mathbf{J}(\mathbf{X}_{ijk}) \cdot \mathbf{n} A = \sum_{r=1}^4 \mathbf{B}_r \cdot d\mathbf{x}_r$$

$$\mathbf{J}(\mathbf{X}_U) \approx \mathbf{J}(\mathbf{X}_{ijk}), \quad \mathbf{X}_U \in U$$

3 planes will give 3 l.i. normal vectors:

$$I^p = \mathbf{J}(\mathbf{X}_{ijk}) \cdot \mathbf{n}^p = \sum_{r=1}^4 \mathbf{B}_r^p \cdot d\mathbf{x}_r / A^p$$



$$\nabla_M \times \nabla_M \phi = 0$$

Inversion yields  $\mathbf{J}$  with  $\nabla \cdot \mathbf{J} = 0$ .

(Hyman, Shashkov 1997)

$$\nabla_M \cdot \nabla_M \times \mathbf{A} = 0$$

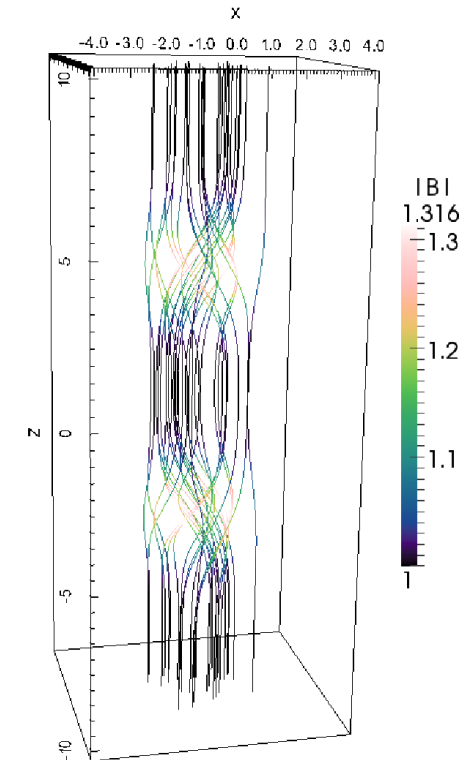
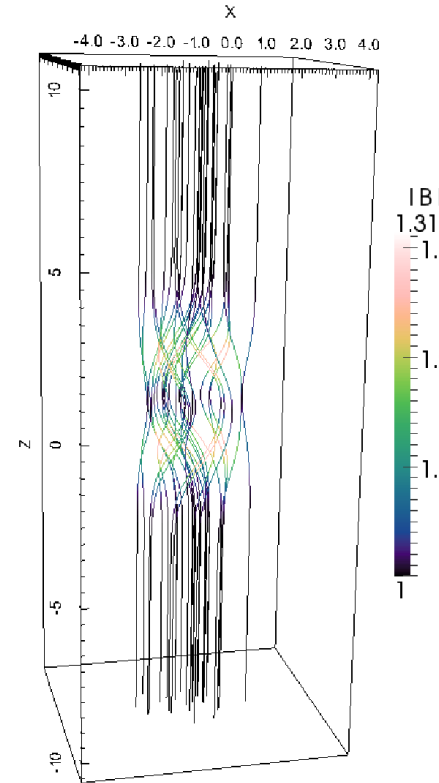
# Simulations

- GPU code GLEMuR (**Gpu-based Lagrangian mimetic Magnetic Relaxation**)
  - line tied boundaries
  - mimetic vs. classic

*(Candelaresi et al. 2014)*



Nvidia Tesla K40



we know:

$$\lim_{t \rightarrow \infty} \mathbf{B}(t)$$

$$\lim_{t \rightarrow \infty} \mathbf{x}(t)$$

we know:

$$\lim_{t \rightarrow \infty} \mathbf{B}(t)$$

# Quality Parameters

Deviation from the expected relaxed state:

$$\sigma_{\mathbf{x}} = \sqrt{\frac{1}{N} \sum_{ijk} (\mathbf{x}(\mathbf{X}_{ijk}) - \mathbf{x}_{\text{relax}}(\mathbf{X}_{ijk}))^2}$$

$$\sigma_{\mathbf{B}} = \sqrt{\frac{1}{N} \sum_{ijk} (\mathbf{B}(\mathbf{X}_{ijk}) - \mathbf{B}_{\text{relax}}(\mathbf{X}_{ijk}))^2}$$

Free magnetic energy:

$$E_{\text{M}}^{\text{free}} = E_{\text{M}} - E_{\text{M}}^{\text{bkg}}$$

$$E_{\text{M}} = \int_V \mathbf{B}^2 / 2 \, dV \quad \mathbf{B}^{\text{bkg}} = B_0 \hat{e}_z$$

# Quality Parameters

For a force-free field:  $\nabla \times \mathbf{B} = \alpha \mathbf{B}$

$$\mathbf{B} \cdot \nabla \alpha = 0$$

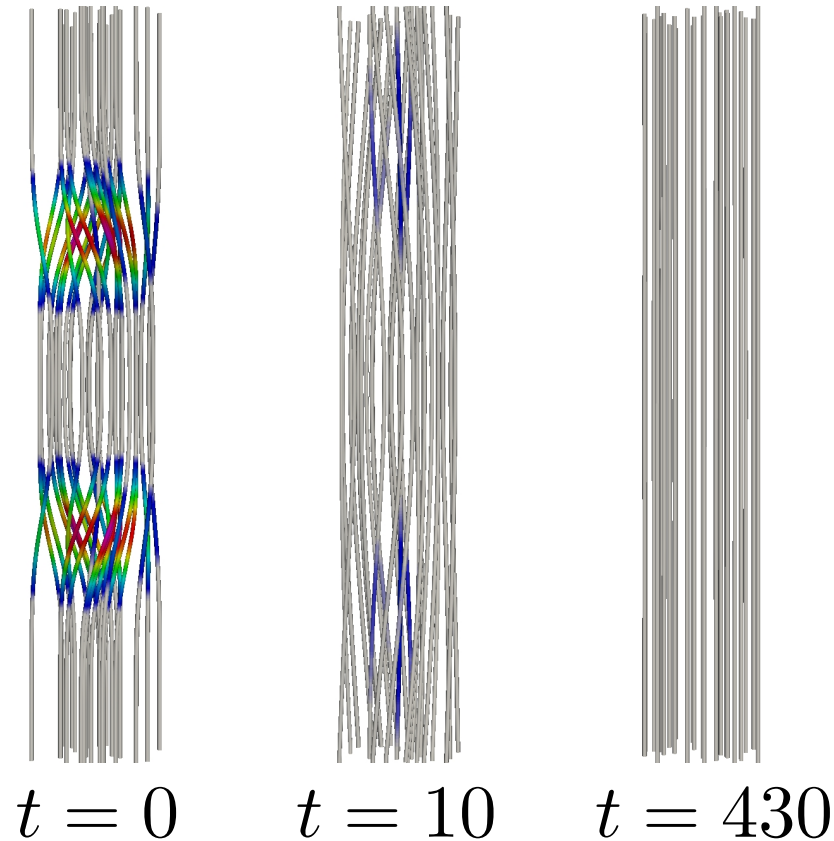
- Force-free parameter does not change along field lines.
- Measure the change of  $\alpha^* = \frac{\mathbf{J} \cdot \mathbf{B}}{\mathbf{B}^2}$  along field lines:

$$\epsilon^* = \max_{i,j} \left( a_r \frac{\alpha^*(\mathbf{X}_i) - \alpha^*(\mathbf{X}_j)}{|\mathbf{X}_i - \mathbf{X}_j|} \right); \quad \mathbf{X}_i, \mathbf{X}_j \in s_\alpha$$

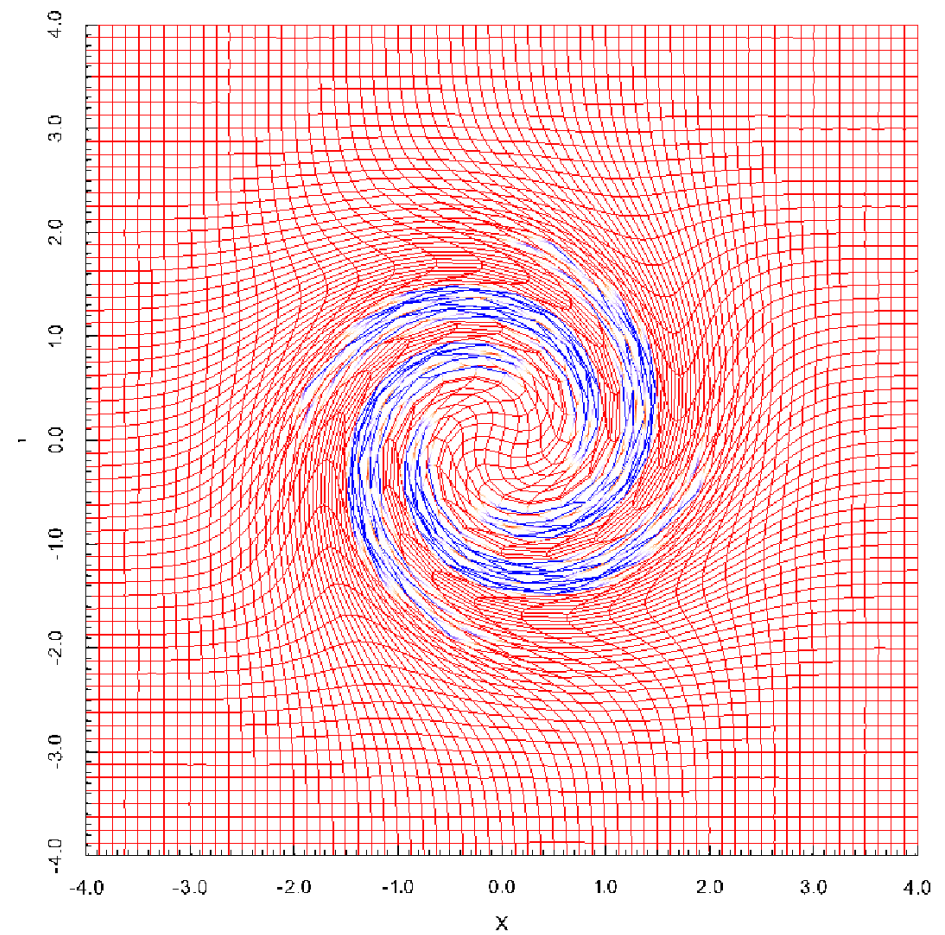
Particular field line:  $s_\alpha = \{(0, 0, Z) : Z \in [-L_z/2, L_z/2]\}$

# Field Relaxation

Magnetic streamlines:

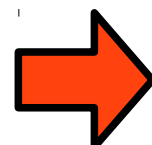
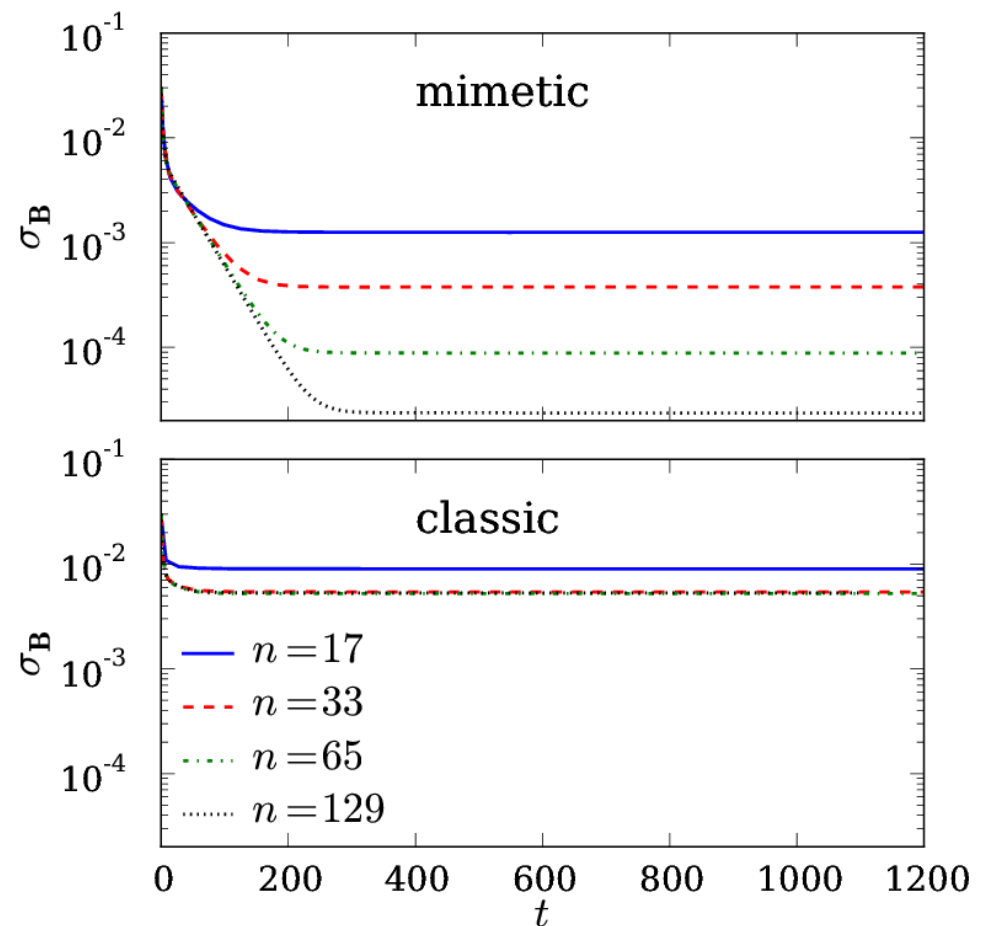
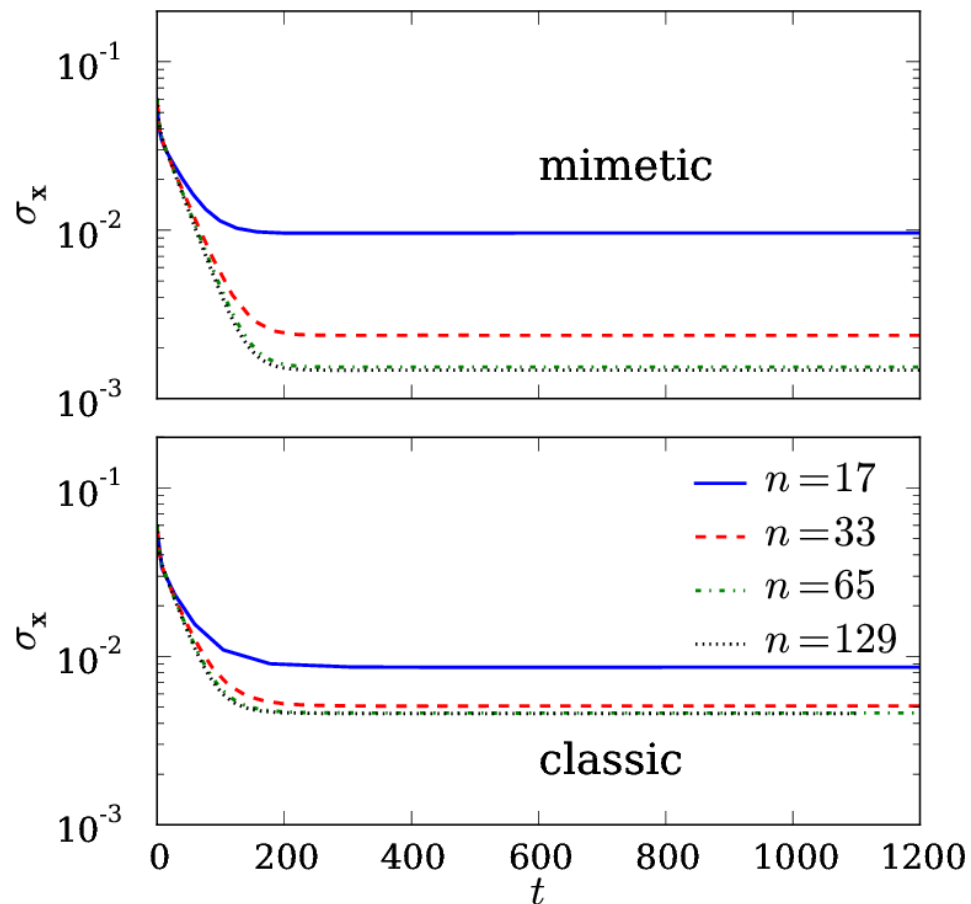


Grid distortion at mid-plane:



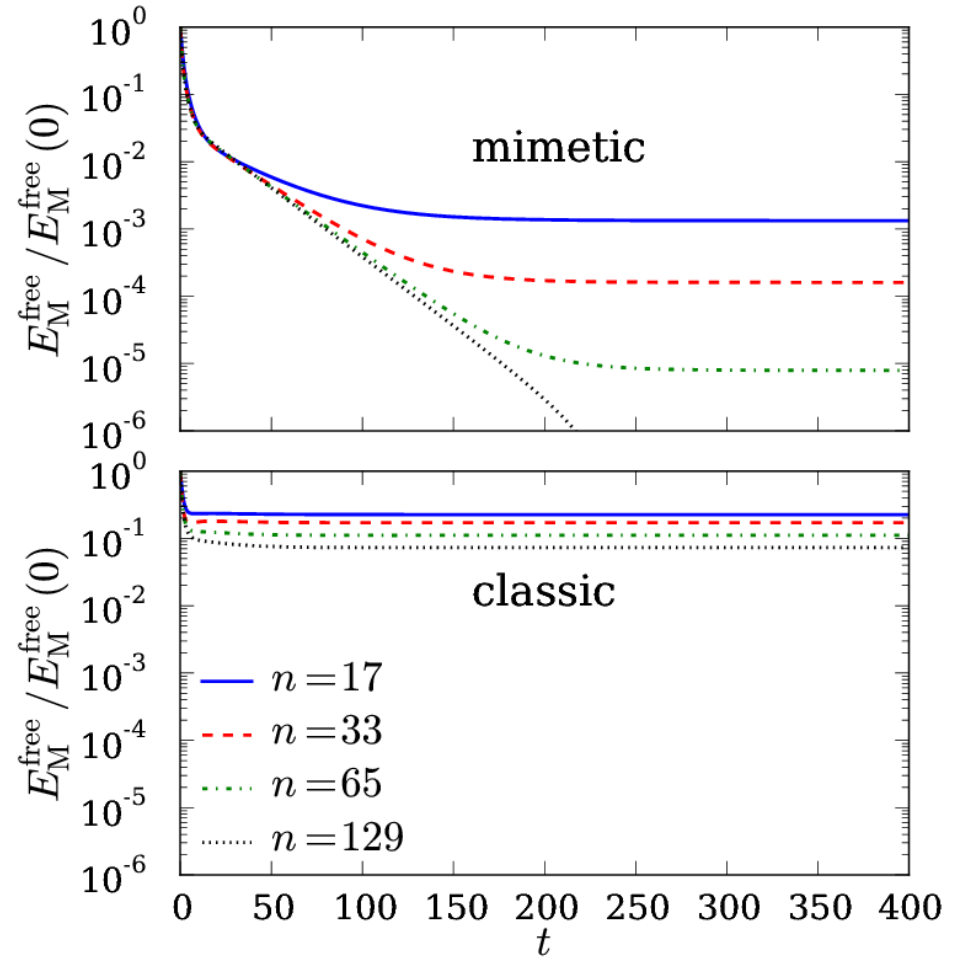
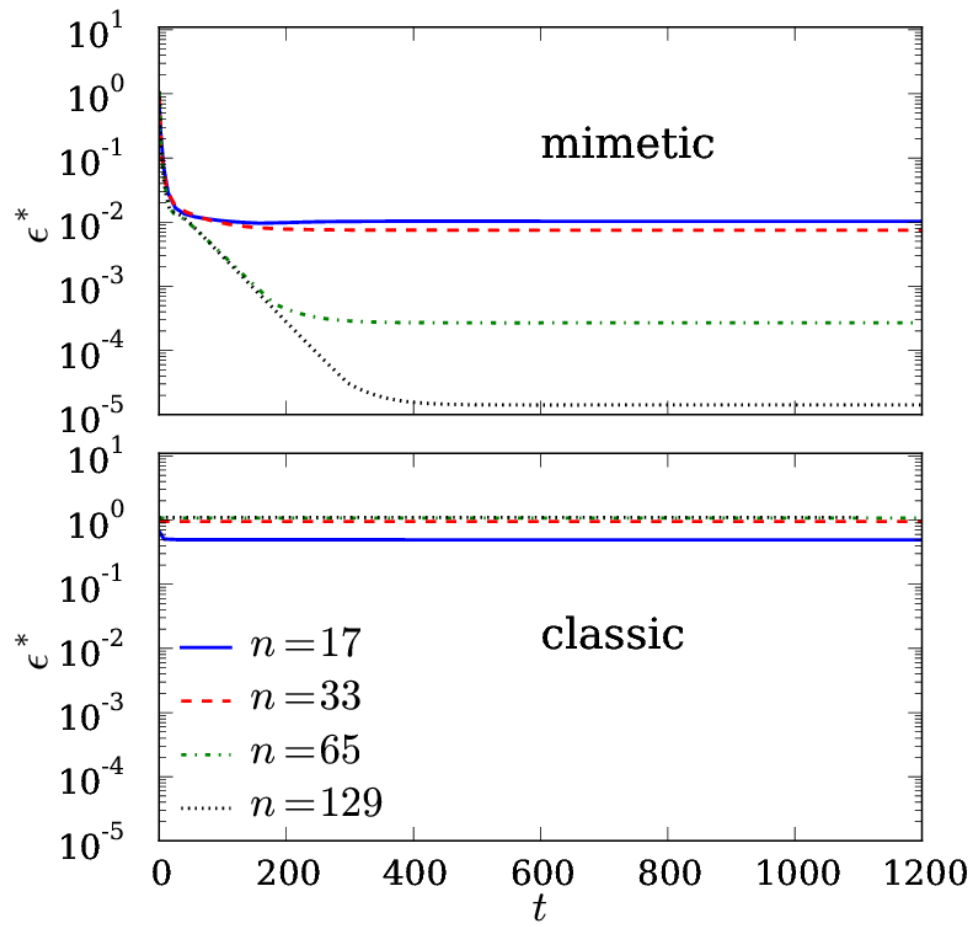
movie

# Relaxation Quality



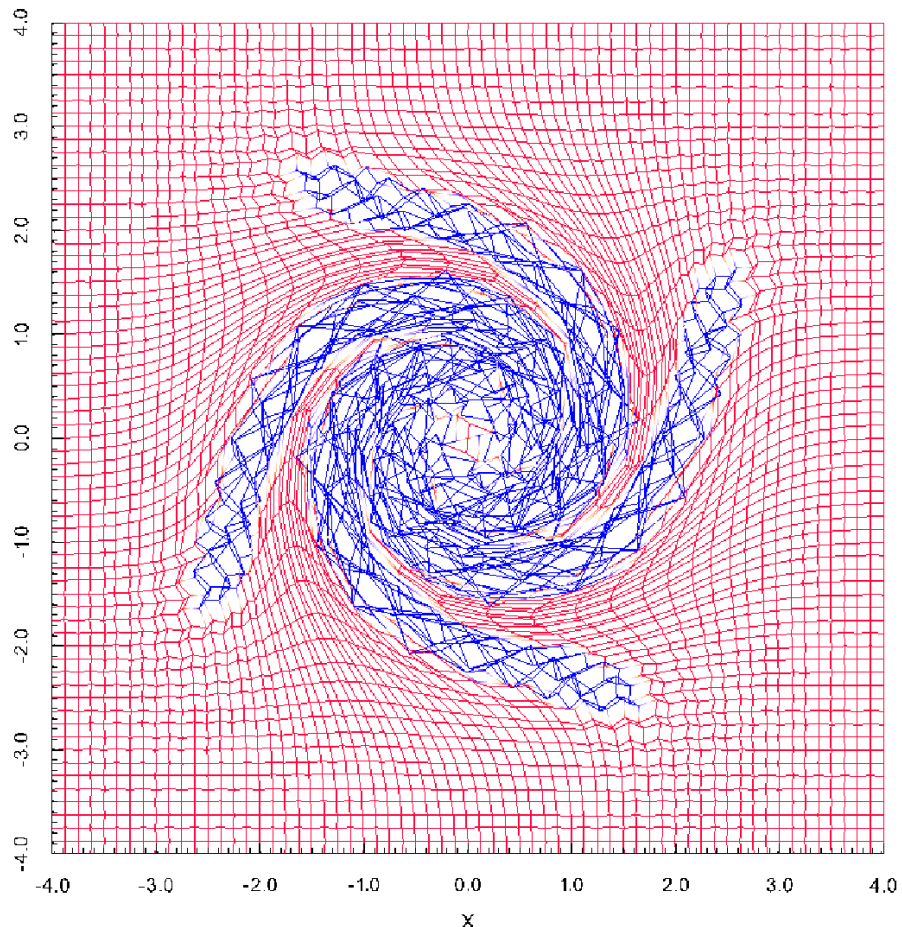
Closer to the analytical solution by 3 orders of magnitude.

# Relaxation Quality



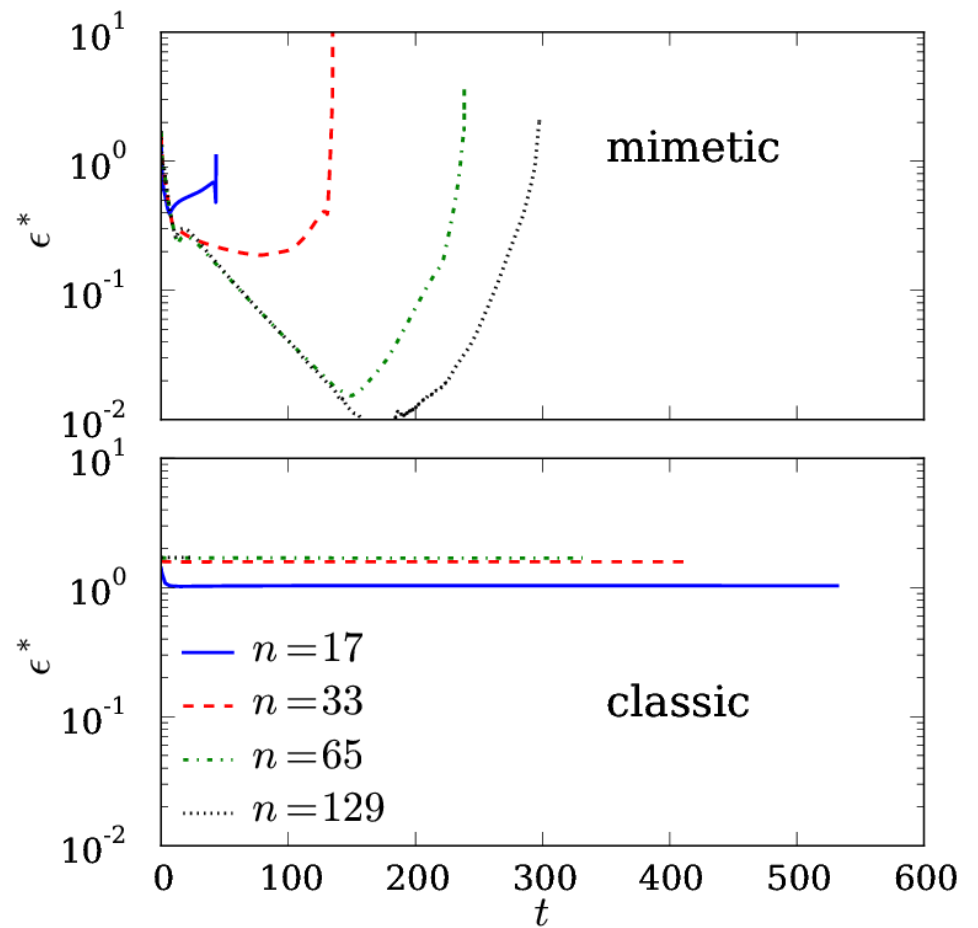
Closer to force-free state by 5 orders of magnitude.

# Limitations



red: convex  
blue: concave

For concave cells the method becomes unstable.  
**But:** results before crash better than classic method.



# Code Details

-  written in C++
-  6<sup>th</sup> order Runge-Kutta time stepping
-  running in GPUs
-  periodic and line-tied boundaries
-  VTK data format
-  post processing routines in Python

```
// compute the norm of JxB/B**2
__global__ void JxB_B2(REAL *B, REAL *J, REAL *JxB_B2, int dimX, int dimY, int dimZ) {
    int i = threadIdx.x + blockDim.x * blockIdx.x;
    int j = threadIdx.y + blockDim.y * blockIdx.y;
    int k = threadIdx.z + blockDim.z * blockIdx.z;
    int p = threadIdx.x;
    int q = threadIdx.y;
    int r = threadIdx.z;
    int l;
    REAL B2;

    // shared memory for faster communication, the size is assigned dynamically
    extern __shared__ REAL s[];
    REAL *Bs = s;                                // magnetic field
    REAL *Js = &s[3 * dimX * dimY * dimZ];        // electric current density
    REAL *JxBs = &Js[3 * dimX * dimY * dimZ];      // JxB

    // copy from global memory into shared memory
    if ((i < dev_p.nx) && (j < dev_p.ny) && (k < dev_p.nz)) {
        for (l = 0; l < 3; l++) {
            Bs[l + p*3 + q*dimX*3 + r*dimX*dimY*3] = B[l + (i+1)*3 + (j+1)*(dev_p.nx+2)*3 + (k+1)*(dev_p.nx+2)*(dev_p.ny+2)*3];
            Js[l + p*3 + q*dimX*3 + r*dimX*dimY*3] = J[l + i*3 + j*dev_p.nx*3 + k*dev_p.nx*dev_p.ny*3];
        }

        cross(&Js[0 + p*3 + q*dimX*3 + r*dimX*dimY*3],
              &Bs[0 + p*3 + q*dimX*3 + r*dimX*dimY*3],
              &JxBs[0 + p*3 + q*dimX*3 + r*dimX*dimY*3]);
    }

    B2 = dot(&Bs[0 + p*3 + q*dimX*3 + r*dimX*dimY*3], &Bs[0 + p*3 + q*dimX*3 + r*dimX*dimY*3]);

    // return result into global memory
    JxB_B2[i + j*dev_p.nx + k*dev_p.nx*dev_p.ny] = norm(&JxBs[0 + p*3 + q*dimX*3 + r*dimX*dimY*3])/B2;
}
}
```

# Similarities with the PencilCode

## Fortran name lists

```
&comp
    nx = 33;  ny = 33;  nz = 33
/
&start
    Lx = 0.6;      Ly = 0.6;      Lz = 1.0
    Ox = -0.3;     Oy = -0.3;     Oz = -0.5
    bInit = "sheared"
    ampl = 1.
    initDist = "initShearX"
    initShear0 = 0.7
    initShearK = 1.
    fRestart = t
/
```

## Bash commands

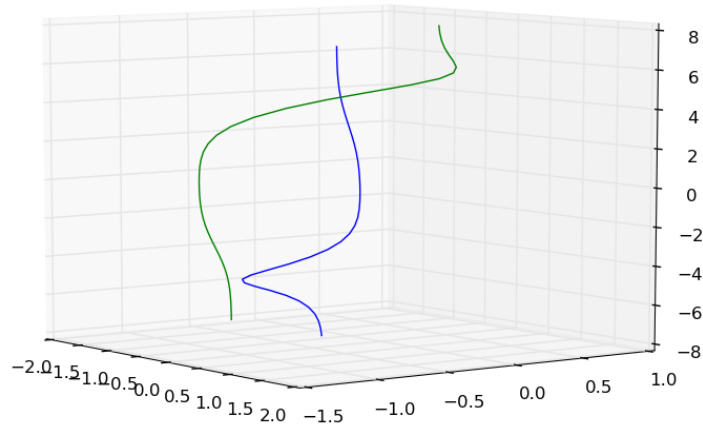
```
gm_ci_run
gm_inspectrun
gm_newrun
```

## time\_series.dat

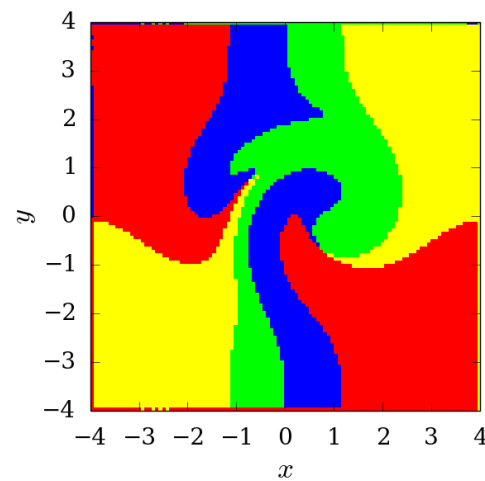
#	it	t	dt	maxDelta	JxB_B2Max	epsilonStar	B2	convex
0	1.29540e-06	1.29540e-06	1.78814e-07	1.50932e+02	2.81160e+02	7.12394e-01	-1.00000e+00	
1	3.08508e-06	1.78967e-06	1.19209e-07	1.13175e+02	2.96738e+02	7.12170e-01	-1.00000e+00	
2	5.76647e-06	2.68139e-06	1.78814e-07	8.83429e+01	3.15884e+02	7.11882e-01	-1.00000e+00	
3	9.47096e-06	3.70449e-06	1.19209e-07	7.67879e+01	3.36120e+02	7.11536e-01	-1.00000e+00	
4	1.50212e-05	5.55028e-06	1.78814e-07	6.44194e+01	3.57402e+02	7.11085e-01	-1.00000e+00	
5	2.13638e-05	6.34253e-06	7.74860e-07	5.44002e+01	3.73753e+02	7.10636e-01	-1.00000e+00	

# Post-Processing

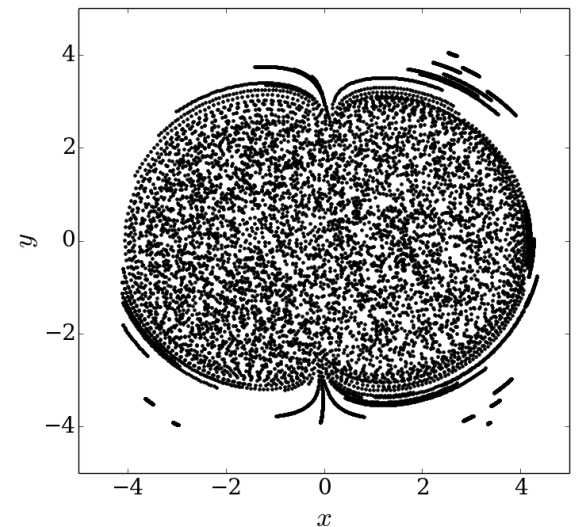
streamlines



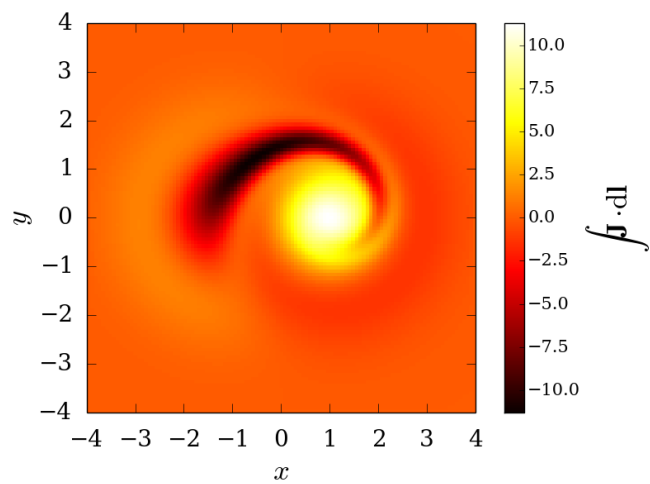
field line mapping



Poincaré maps



line integration



save and read as vtk file

```
s0 = gm.streamInit(tol = 0.01)
```



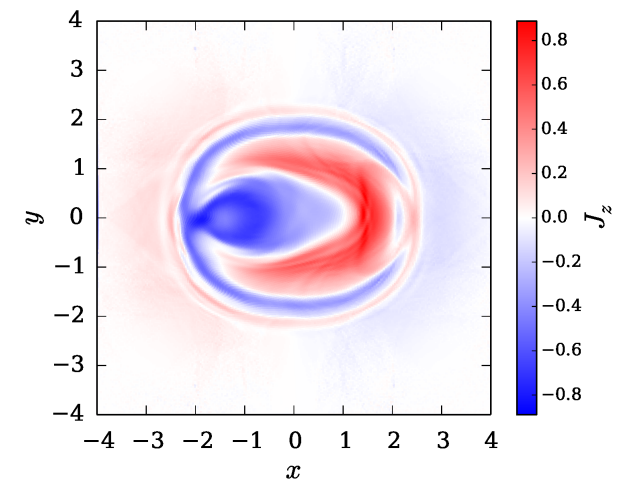
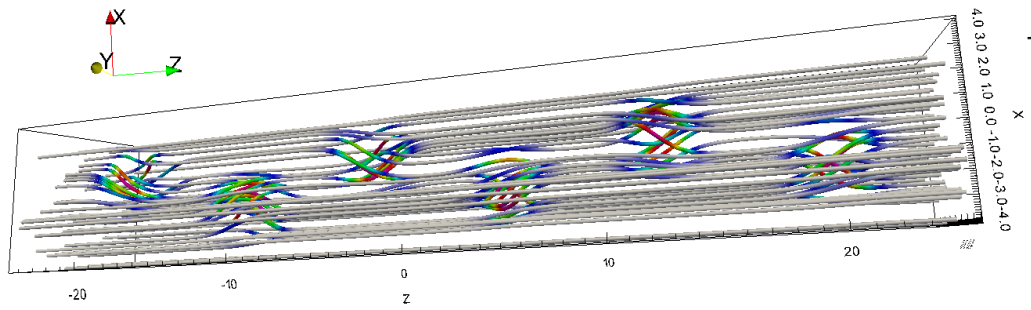
```
stream.vtk
```



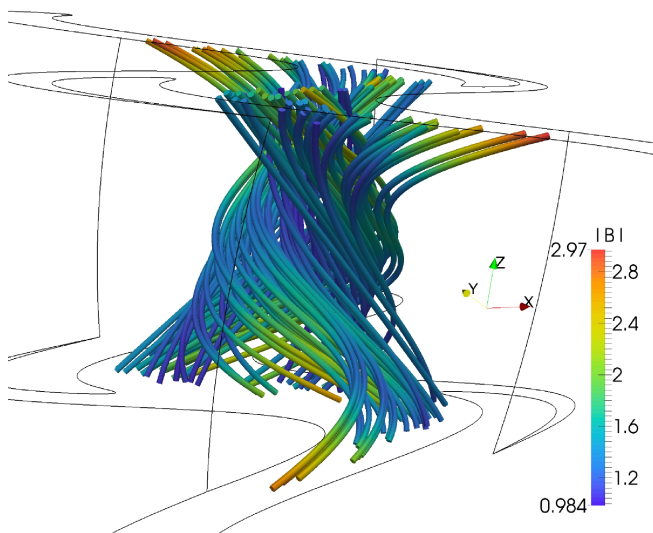
```
sr = gm.readStream()
```

# Current Structures

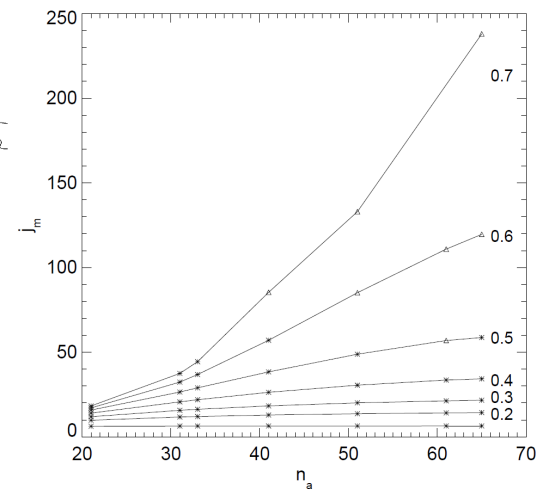
Braided fields:



Sheared fields:

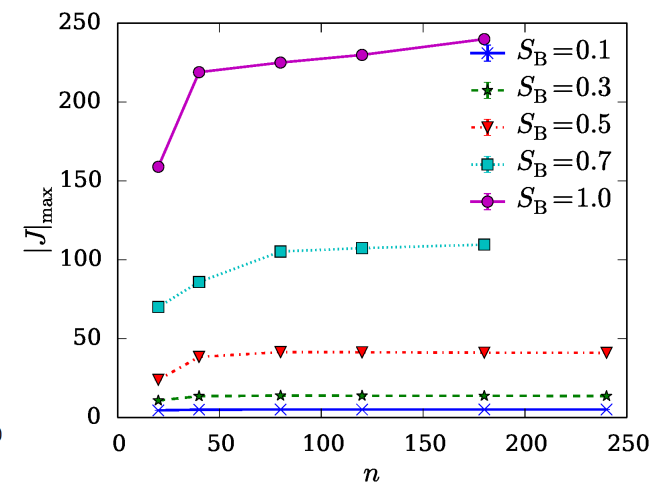


then:



*Longbottom (1998)*

now:



# Conclusions

- Lagrangian numerical scheme for ideal evolution.
- Preserving field line topology.
- Mimetic methods more capable of producing force-free fields.
- GLEMuR code running on GPUs.
- No evidence for current sheets in sheared and braided setups

[simon.candelaresi@gmail.com](mailto:simon.candelaresi@gmail.com)

[www.maths.dundee.ac.uk/scandelaresi/](http://www.maths.dundee.ac.uk/scandelaresi/)

[www.youtube.com/user/iomsn/videos](http://www.youtube.com/user/iomsn/videos)